

## The Journal of The Textile Institute

Publication details, including instructions for authors and subscription information:

<http://www.tandfonline.com/loi/tjti20>

### A novel method for the identification of weave repeat through image processing

F. Ajallouian <sup>a</sup> , H. Tavanai <sup>a</sup> , M. Palhang <sup>b</sup> , S. A. Hosseini <sup>a</sup> , S. Sadri <sup>b</sup> & K. Matin <sup>a</sup>

<sup>a</sup> Department of Textile Engineering , Isfahan University of Technology , Isfahan, 84156-83111, Iran

<sup>b</sup> Department of Electrical and Computer Engineering , Isfahan University of Technology , Isfahan, 84156-83111, Iran

Published online: 22 Apr 2009.

To cite this article: F. Ajallouian , H. Tavanai , M. Palhang , S. A. Hosseini , S. Sadri & K. Matin (2009) A novel method for the identification of weave repeat through image processing, *The Journal of The Textile Institute*, 100:3, 195-206, DOI:

[10.1080/00405000701660244](https://doi.org/10.1080/00405000701660244)

To link to this article: <http://dx.doi.org/10.1080/00405000701660244>

PLEASE SCROLL DOWN FOR ARTICLE

Taylor & Francis makes every effort to ensure the accuracy of all the information (the "Content") contained in the publications on our platform. However, Taylor & Francis, our agents, and our licensors make no representations or warranties whatsoever as to the accuracy, completeness, or suitability for any purpose of the Content. Any opinions and views expressed in this publication are the opinions and views of the authors, and are not the views of or endorsed by Taylor & Francis. The accuracy of the Content should not be relied upon and should be independently verified with primary sources of information. Taylor and Francis shall not be liable for any losses, actions, claims, proceedings, demands, costs, expenses, damages, and other liabilities whatsoever or howsoever caused arising directly or indirectly in connection with, in relation to or arising out of the use of the Content.

This article may be used for research, teaching, and private study purposes. Any substantial or systematic reproduction, redistribution, reselling, loan, sub-licensing, systematic supply, or distribution in any form to anyone is expressly forbidden. Terms & Conditions of access and use can be found at <http://www.tandfonline.com/page/terms-and-conditions>

## A novel method for the identification of weave repeat through image processing

F. Ajallouian<sup>a</sup>, H. Tavanai<sup>a\*</sup>, M. Palhang<sup>b</sup>, S.A. Hosseini<sup>a</sup>, S. Sadri<sup>b</sup> and K. Matin<sup>a</sup>

<sup>a</sup>Department of Textile Engineering, Isfahan University of Technology, Isfahan 84156-83111, Iran;

<sup>b</sup>Department of Electrical and Computer Engineering, Isfahan University of Technology, Isfahan 84156-83111, Iran

(Received 28 January 2007; final version received 8 September 2007)

Conventionally, weave repeat is identified manually by extracting individual warp or weft yarns from the fabric. This process can be troublesome and time-consuming. Therefore, automatic methods capable of identifying woven fabric repeat can be very useful.

This paper describes the application of a new algorithm using image processing techniques for the development of an automatic method, capable of identifying weave repeat. This method is based on scanning and obtaining a gray scale image of the original sample and enhancing it by morphological operations. The enhanced image is filtered by steerable vertical filters and then segmented into blocks showing either a warp or a weft point. The blocked image is divided into specific sub images, followed by operating sum over their columns and forming a matrix from them. A primary and secondary threshold is then defined giving rise to the formation of the weave pattern in the form of black and white squares. To identify the weave repeat, a matrix, replacing the black and white squares of the weave pattern by zero and one is produced. Then the first repeating row and column are found, showing the start of the next repeat vertically and horizontally, leading to the identification of weave repeat.

**Keywords:** weave repeat; image analysis; morphological operations; steerable filters; nonlinear diffusion filtering; fuzzy c-means clustering

### Introduction

The weave repeat of any woven fabric can be defined as a specific array of a certain number of warp and weft points in the form of a square or rectangle, repeating itself in the width and length directions of the fabric. Warp point shows the warp crossing over the weft and vice versa. The reproduction of a woven fabric requires the identification of its weave repeat, so that the correct drawing-in, shed formation and weft insertion can be carried out. This guarantees the correct reproduction of the original weave.

Conventionally, weave repeat is identified by extracting the individual warp or weft yarns manually from the fabric and determining whether warp is crossing weft or vice versa at each crossing point. Simultaneously, a space on a point paper is or is not marked for a warp crossing weft or a weft crossing warp accordingly. The marking of the point paper must continue until the repeat is recognized. For complex weaves, it may be necessary to continue marking until the obtained pattern contains just over two repeats vertically and horizontally. For many basic and simple weaves, it is enough to mark the point paper until the first row and column starts repeating itself. Then the repeat can be identified. The manual repeat identification can be tiring and time consuming, especially for dense fabrics and complex weaves.

Therefore, automatic methods capable of identifying weave repeat can be very useful.

Basic weaves, i.e., plain, twill, and satin have a square form repeat. Plain weave, which is the simplest, has only one kind of repeat but twill and satin have different kinds. Basic weaves can be expanded leading to new repeats. Twill and satin can also have derivatives. Warp rib, weft rib, and panama are examples of plain weave expansion.

This paper describes a novel algorithm, using image processing techniques, leading to an automatic method, capable of identifying any weave repeat.

### Literature review

The basic research in the area of weave repeat identification has focused on Fourier transform techniques, making use of the peaks in the related power spectrum image, in order to extract frequency terms of periodic elements (Ravandi & Toriumi, 1995; Xu, 1996). Although this technique can identify basic weaves, it is not capable of discriminating different kinds of twill or satin weaves. Xu, (1996) using Fourier transform, employed the lines and their directions for the identification of different weaves from each other. Kang, Kim, and Oh (1999) identified crossing points first, followed by their separation into warp or weft points and finally the color of each warp or weft point. Ohta, Nonaka,

\*Corresponding author. Email: tavanai@cc.iut.ac.ir

and Miyawaki (1995) converted a CCD image to a digital one and tried to identify weaves with the help of transmitted and reflected images. Huang, Liu, and Yu (2000) employed the maximum and minimum of the sum of lines of the vertical and horizontal pixels of the image to determine crossover points and then using area geometric shape, determined warp or weft floats. Lachkar, Benslimane, Dorazio, and Martuscelli (2005) used inverse of Fourier transform and thinning operator to obtain the borders of the yarns, identifying only the plain weave. It is reminded that these methods are very sensitive to gray value changes in both horizontal and vertical directions and as a result, may not give good results.

Neural networks and Fuzzy logic have also been used as a means of identifying weaves (Jeon, Bae, & Suh, 2003; Kuo, Shih, & Lee, 2004). The result of these works, like those already explained, is also limited to identifying only basic weaves but not the exact weave repeat.

To the best of authors' knowledge, no automatic method capable of identifying any weave repeat has been developed up to now.

### Theoretical background

Digital image processing is a means of modifying digital images with the aims such as enhancing image quality in time or frequency domain, image restoration, image compression, etc. The technique of digital image processing has found increasing importance in many research activities as a powerful and useful technique (Gonzales & Wintz, 1987). Image processing supports three kinds of images, i.e. binary, intensity, and color. Linear and nonlinear operators constitute two important approaches of image processing with the aim of manipulating the image for further work.

Linear systems such as steerable filtering, along with nonlinear ones such as morphological operations and nonlinear diffusion filtering constitute the basic theories employed in this research, with the aim of enhancing the scanned images of the woven fabrics as well as determining crossover points or floats. It must be pointed out that linear systems such as low pass filters including average, median, and Gaussian were used for this purpose, but in spite of their good ability to reduce noise, they were not considered suitable because the sharpness of the edges, in other words, the variation of the light intensity in the edge and neighboring areas, was reduced. Light intensity difference plays an important role when the scanned image undergoes processing. Moreover, even linear based high pass filters such as Sobel, Prewitt, Laplacian of Gaussian and Canny proved to be inefficient. It must be pointed out that the quality of the scanned images of the fabrics obtained from the scanner mentioned in the instrument part of this paper was good enough to be successfully processed.

### Gray-level morphology

Mathematical morphology, which has originally been developed for binary images, uses set-theoretic operations

such as union, intersection, and set complement extensively. Furthermore, translation plays a major role in this classical morphology. Later, the theory extended to gray-level images. Gray-level images can be thought of in three dimensions, so that  $x$  and  $y$  axes represent pixel positions and the  $z$  axis represents the intensity of each pixel. In other words, the image is viewed as a surface, with mountain (high intensity) and valleys (low intensity). The contrast can be improved by minimizing the number of valleys. The top-hat image contains the "peaks" of objects that fit the structuring element. Hence, the residual between original image and opened image can be defined as top-hat transform. In contrast, the bottom-hat image shows the gaps between the objects of interest. In fact, the residual between closed image and original image is denoted bottom-hat transform. To maximize the contrast between the objects and the gaps that separate them from each other, the bottom-hat image is subtracted from the sum of original and top-hat images (Cui, 1999; Heijmansh, 1991; Parker, 1997).

### Steerable filters

Oriented filters functioning in a specific direction can be used in many image-processing techniques, such as texture analysis, edge detection, image data compression, and image enhancement. Linear filters, on the other hand, can be oriented in all possible directions. Such filters of arbitrary orientation consisting of a linear combination of two-dimensional (2-D) basic filters are called steerable filters. Steerable filters with the following basic 2-D Gaussian function (Equation (1)) are used in this work,

$$f(x, y) = \frac{1}{2\pi\sigma_x\sigma_y} \exp\left[-\left(\frac{x^2}{2\sigma_x^2} + \frac{y^2}{2\sigma_y^2}\right)\right] \quad (1)$$

where  $\sigma_x$  and  $\sigma_y$  are the standard deviation in the  $x$  and  $y$  directions, respectively.

In order to introduce the rotation angle ( $\theta$ ) at the position  $X = (x, y)$  into the function, we use the rotation matrix to rotate the axis according to desired angle (Equation (2)).

$$\begin{bmatrix} X \\ Y \end{bmatrix} = \begin{bmatrix} \cos \theta & \sin \theta \\ -\sin \theta & \cos \theta \end{bmatrix} \begin{bmatrix} x \\ y \end{bmatrix} \quad (2)$$

So, the steerable filter is obtained as Equation (3), and after defining suitable parameters of  $\sigma_x$ ,  $\sigma_y$ ,  $\theta$  the filter is convolved with corresponding enhanced image (Freeman, 1992; Freeman & Adelson, 1991).

$$f(x, y) = \frac{1}{2\pi\sigma_x\sigma_y} \exp \times \left[ -\frac{(x \cos \theta + y \sin \theta)^2}{2\sigma_x^2} - \frac{(-x \sin \theta + y \cos \theta)^2}{2\sigma_y^2} \right] \quad (3)$$

### Nonlinear diffusion filtering

Noise removal in image processing is very important and is generally done by linear low-pass (isotropic diffusion) filtering. However, as already explained, this leads to less sharp edges. Nonlinear diffusion (anisotropic) filtering has the advantage of preserving the sharpness of the edges throughout the image smoothing process (Edge Preserving Denoising). In this work, nonlinear diffusion filtering is used so that the determination of the first threshold is facilitated. This kind of filtering has been used in conjunction with edge detection. By impeding diffusion at the image edges, anisotropic diffusion which yields intraregion smoothing can be used to retain image features of a specified scale.

The main idea behind anisotropic diffusion is the introduction of a function known as, diffusion coefficient that inhibits smoothing at the image edges. Diffusion coefficient,  $c(x)$ , encourages intraregion smoothing over interregion smoothing. If  $c(x)$  remains constant at all locations, then smoothing progress is isotropic. If  $c(x)$  is allowed to vary according to the local image gradient like Equation (4) (as an example) in which different results are obtained, using different values for  $K$ , smoothing anisotropic diffusion is obtained. This was employed in our work.

$$c(x, t) = \frac{1}{1 + \left| \frac{\nabla I_t(x)}{K} \right|^2} \quad (4)$$

The basic form of anisotropic diffusion is a partial differential equation as Equation (5),

$$\frac{\partial I_t(x)}{\partial t} = \operatorname{div} \{ c(x) \nabla I_t(x) \} \quad (5)$$

where  $I$  represents an image with real-valued intensity  $I(x)$  at position  $x$  and  $I_t$  shows the image at time  $t$  with intensities  $I_t(x)$ . Image intensities are updated according to Equation (6),

$$\{I(x)\}_{t+1} = \left[ I(x) + (\Delta T) \sum_{d=1}^r c_d(x) \nabla I_d(x) \right] \quad (6)$$

where  $r$  is the number of directions in which diffusion is computed,  $\nabla I_d(x)$  is the directional derivative (simple difference) in direction  $d$  at location  $x$ ,  $t$  shows time (in iterations), and  $\Delta T$  is the time step ( $\Delta T \leq 1/2$  in the 1-D case and  $\Delta T \leq 1/4$  in the 2-D case is used for stability).

For 1-D discrete-domain signals (like those we have used in this work) the simple differences  $\nabla I_d(x)$  with respect to the “western” and “eastern” neighbors (neighbors

of the left and right) are defined by Equations (7) and (8),

$$\nabla I_1(x) = I(x - h_1) - I(x) \quad (7)$$

$$\nabla I_2(x) = I(x + h_2) - I(x) \quad (8)$$

where  $h_1$  and  $h_2$  define the sample spacing used to estimate the directional derivatives. For 2-D case, the diffusion directions include the “northern” and “southern” as well as the western and eastern (Bovik, 2000; Perona & Malik, 1990).

### Fuzzy c-means clustering

Clustering is a method for dividing scattered groups of data into several groups. It is commonly viewed as an instance of unsupervised learning. The grouping of patterns is accomplished through clustering by defining and quantifying similarities between the individual data points or patterns. The patterns that are similar to the highest extent are assigned to the same cluster (Pedrycz, 1997). Clustering analysis is based on partitioning a collection of data points into a number of subgroups, where the objects inside a cluster (a subgroup) show a certain degree of closeness or similarity.

Fuzzy c-means is a clustering method, which allows one piece of data to belong to two or more clusters. The fuzzy c-means method (Bezdek, 1981) is frequently used in pattern recognition. It is based on the minimization of the following objective function, with respect to  $U$  and  $V$ :

$$J_m(U, V) = \sum_{j=1}^n \sum_{i=1}^c u_{ij}^m \|X_j - V_i\|^2, \quad 1 \leq m < \infty \quad (9)$$

where  $U$  is a matrix showing the membership degree of instances to different classes,  $V$  is a set of  $C$  prototypes of the data set,  $m$  is any real number greater than 1,  $u_{ij}$  is the membership degree of  $X_j$  in the cluster  $i$ ,  $X_j$  is the  $j$ th member of  $d$ -dimensional measured data,  $V_i$  is the  $d$ -dimensional center of the  $i$ th cluster, and  $\|\cdot\|$  is any norm expressing the similarity between any measured data and the center.

Fuzzy partition is carried out through an iterative optimization of (9) with the update of membership  $u_{ij}$  and the cluster centers  $V_i$  by

$$u_{ij} = \frac{1}{\sum_{k=1}^c \left( \frac{d_{ij}}{d_{ik}} \right)^{\frac{2}{m-1}}} \quad (10)$$

$$V_i = \frac{\sum_{j=1}^n u_{ij}^m X_j}{\sum_{j=1}^n u_{ij}^m} \quad (11)$$

The criteria in this iteration will stop when

$$\max_{ij} \{ \|u_{ij}^{k+l} - u_{ij}^k\| \} < \varepsilon$$

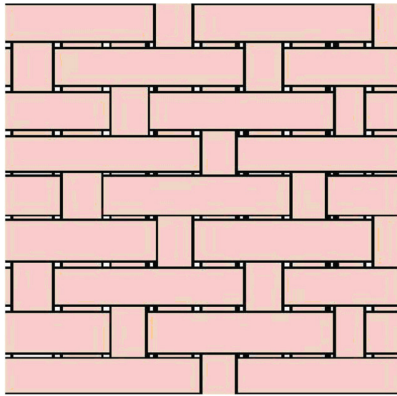


Figure 1. The original ideal image produced by paint showing a weave pattern (9 warp and 9 wefts).

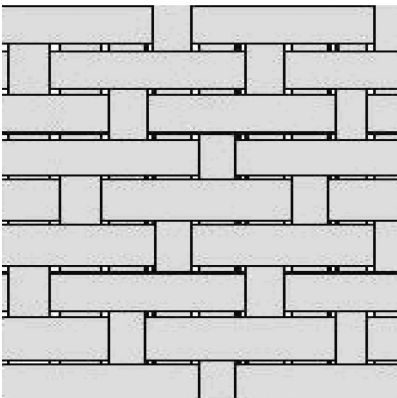


Figure 2. The gray scale image of Figure 1.

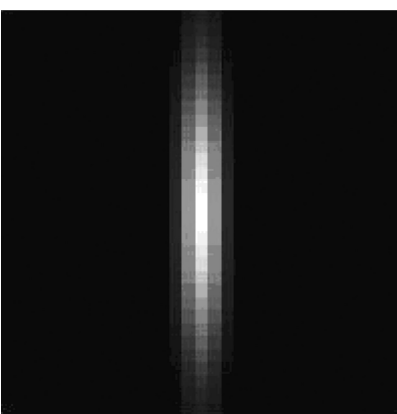


Figure 3. Vertical steerable filter.

$\varepsilon$  is a termination criterion between 0 and 1, whereas  $k$  is the iteration step. This procedure converges to a local minimum or a saddle point of  $J_m$ .

In this paper, we used a fuzzy c-means clustering method to determine the second threshold.

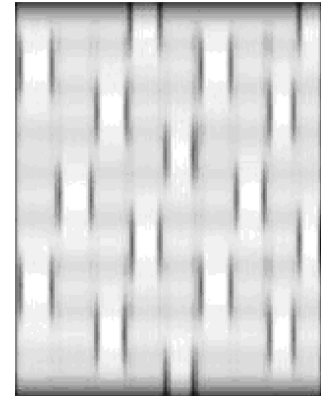


Figure 4. Figure 2 after being filtered vertically.

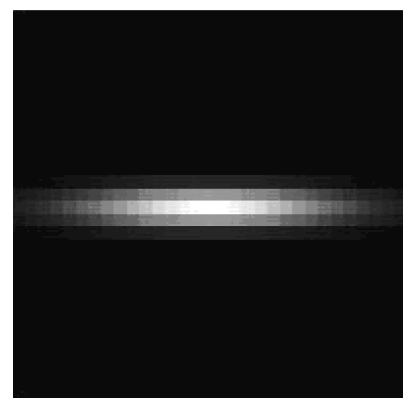


Figure 5. Horizontal steerable filter.

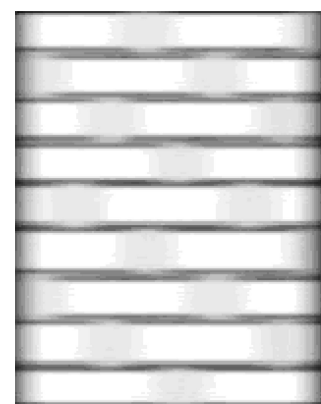


Figure 6. Figure 2 after being filtered horizontally.

### Equipment

PC Pentium 4

Epson scanner 2400 photo

Paint software

Matlab (version 7.1) under windows XP

Different woven fabrics

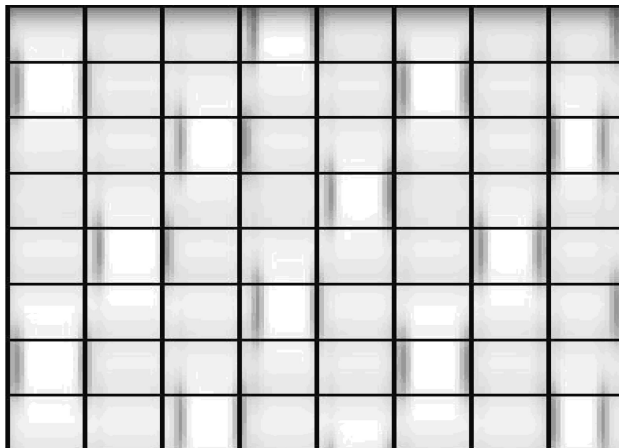


Figure 7. The blocked image of Figure 4.



Figure 8. A sub image of Figure 7 (second from top).

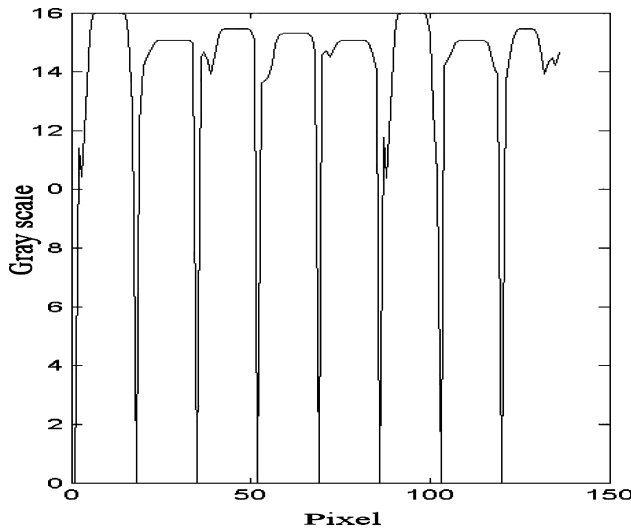


Figure 9. Variation of the sum of the gray scale column versus pixels for Figure 8.

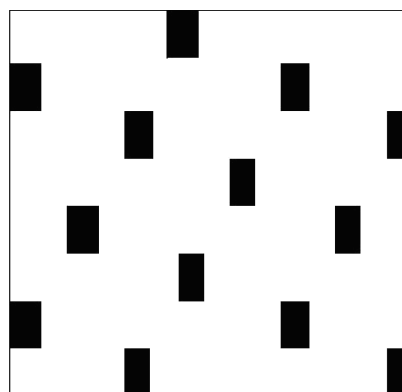


Figure 10. The preliminary weave pattern of Figure 1.

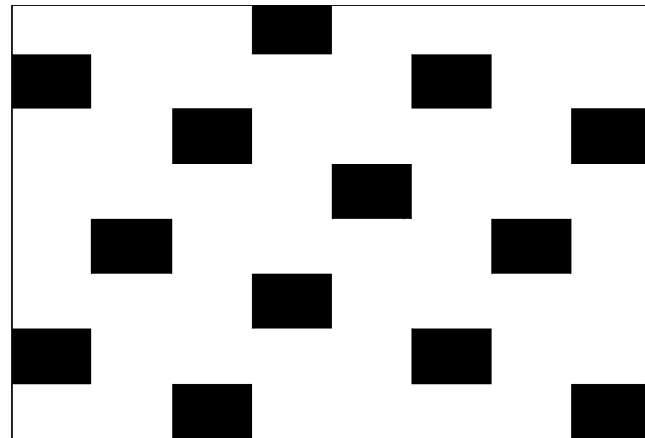


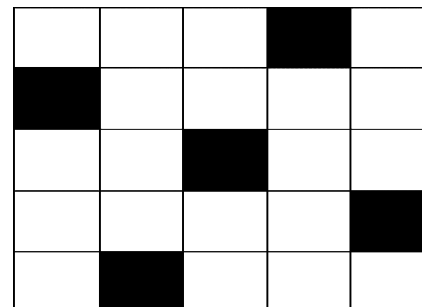
Figure 11. Final weave pattern of Figure 1.

1	1	1	0	1	1	1	1	1
0	1	1	1	1	1	0	1	1
1	1	0	1	1	1	1	1	0
1	1	1	1	0	1	1	1	1
1	0	1	1	1	1	1	0	1
1	1	1	0	1	1	1	1	1
0	1	1	1	1	0	1	1	1
1	1	0	1	1	1	1	1	0

Figure 12. The weave pattern matrix with 0 and 1 replacing the black and white squares in Figure 11.

1	1	1	0	1
0	1	1	1	1
1	1	0	1	1
1	1	1	1	0
1	0	1	1	1

Figure 13. Matrix of weave repeat.

Figure 14. The weave repeat of Figure 1 (Satin  $S_4^1 Z^2$ ).

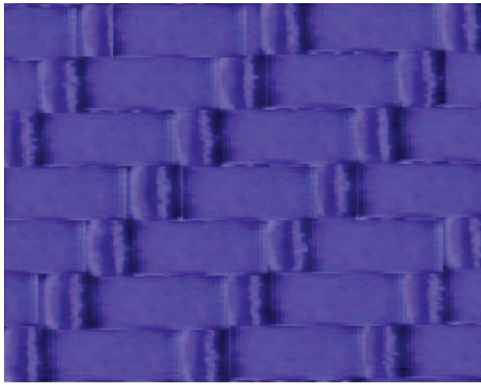


Figure 15. The scanned image (Resolution = 1200 dpi) of a real blue woven fabric. Warp (510 Tex) density = 11 per cm. Weft (412 Tex) density = 11 per cm.

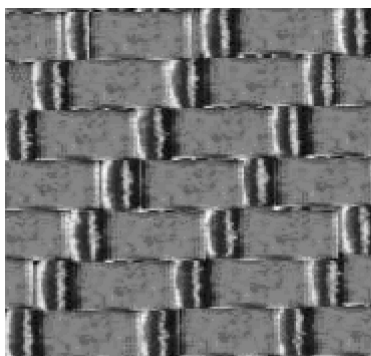


Figure 16. The gray scale image of Figure 15.

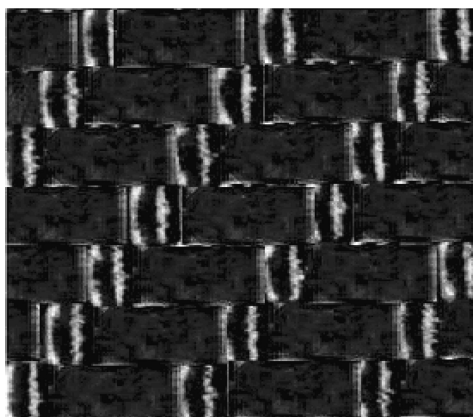


Figure 17. Figure 16 after being operated by top hat.

## Discussion and results

Based on the above theoretical background, the new method developed in our research is explained for ideal and real weaves separately. The procedure for the ideal weaves is somewhat easier than the real ones.

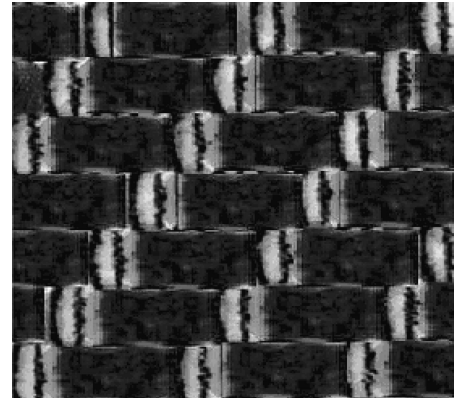


Figure 18. Figure 16 after being operated by bottom hat.

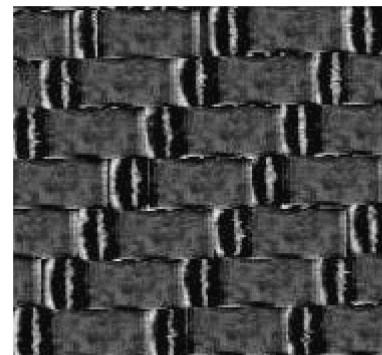


Figure 19. The image resulting from subtracting the bottom-hat image (Figure 18) from sum of top-hat operated image and the original gray scale.

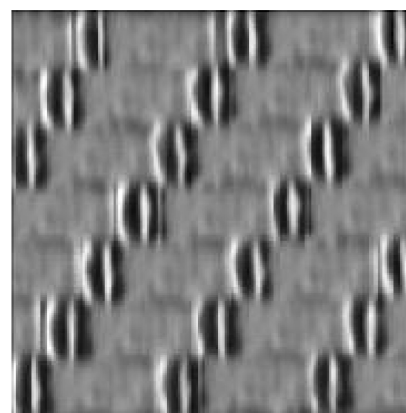


Figure 20. Figure 19 after being operated by vertical steerable filter.

### *Ideal patterns*

Ideal patterns were produced using paint software. An example is shown in Figure 1. It is assumed that the vertical axis of the pattern shows the warp direction. This image, considered as the original one, is transferred into a gray

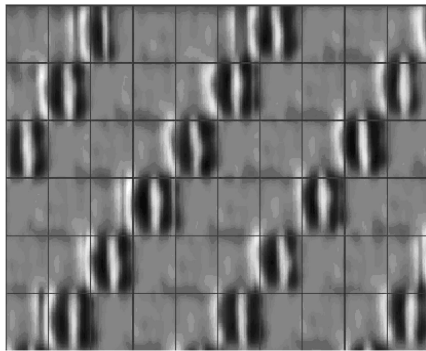


Figure 21. The blocked image of Figure 20.



Figure 22. Sub image of Figure 21.

scale as shown in Figure 2, and subsequently filtered by steerable vertical filter, emphasizing on vertical lines (i.e., warp borders). Figures 3 and 4 show the vertical steerable filter and the result of applying vertical filter on Figure 2, respectively. Figures 5 and 6 show the horizontal steerable filter and Figure 2 after being filtered horizontally, respectively. Both filtered images can be used in the next steps, but in order to generalize the algorithm steps, only the vertical steerable filtered images were selected and then segmented into blocks (Figure 7), each block showing either a warp or a weft point.

To get the blocked image, the width of warp and weft yarns should be obtained. To get these values, the number of warps and wefts *on* the image is counted *manually*. Then, using Matlab, the number of pixels in each row and column of the image is obtained. The number of row pixels is divided by the number of wefts, and the number of column pixels is divided by the number of warps. Since the last warp or weft may not be perfect in the image, a sub image is extracted in which the last warp and weft have been removed (Figure 7). From this blocked image different sub images are extracted, each showing a blocked weft. Figure 8 shows the sub image corresponding to the second weft.

For all sub images, sum operation is carried out vertically, in other words, gray scale values existing in each column are added up so that the number of resulting data in each sub image is equal to the number of pixels in that image column. As a result, a matrix is obtained in which the number of rows is equal to the number of wefts and the number of columns is equal to the number of warps. Then according to similar variations of gray scale values in all sub images, one of them (e.g., the second one) is selected and its variations in terms of gray scale values is plotted against the number of pixels (Figure 9). A primary threshold is obtained from Figure 9. As it can be seen from Figure 9, the primary threshold in this case is 15.7. Comparing primary threshold value of 15.7 with the values of the matrix sum and considering values of either zero or one for each individual pixels of the matrix of the blocked gray scale image as well as their local position making the sum matrix (Figure 7), leads to the formation of a matrix showing warp

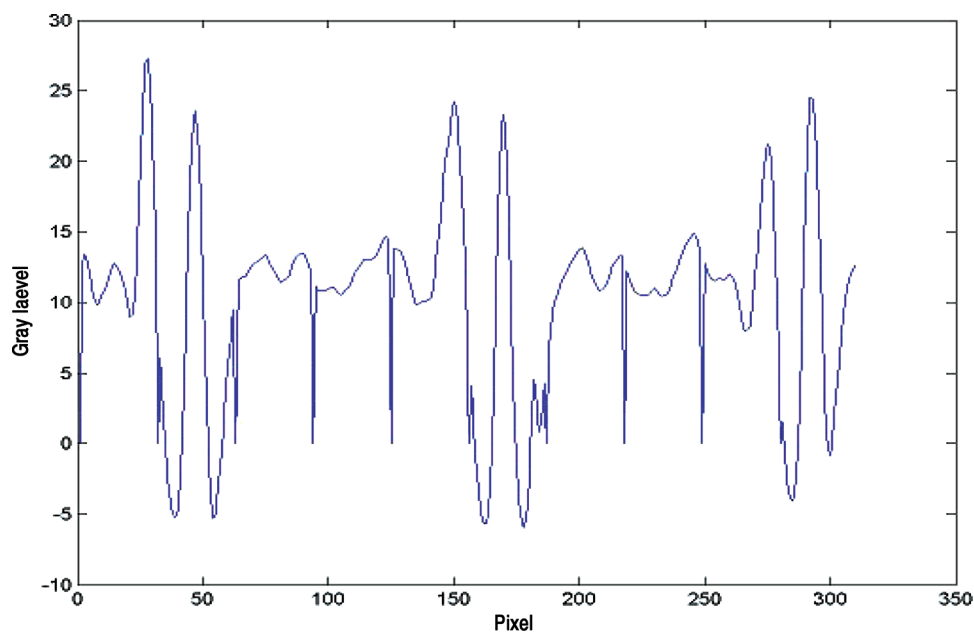


Figure 23. The variation of the sum of the gray scale column versus pixel for Figure 22.

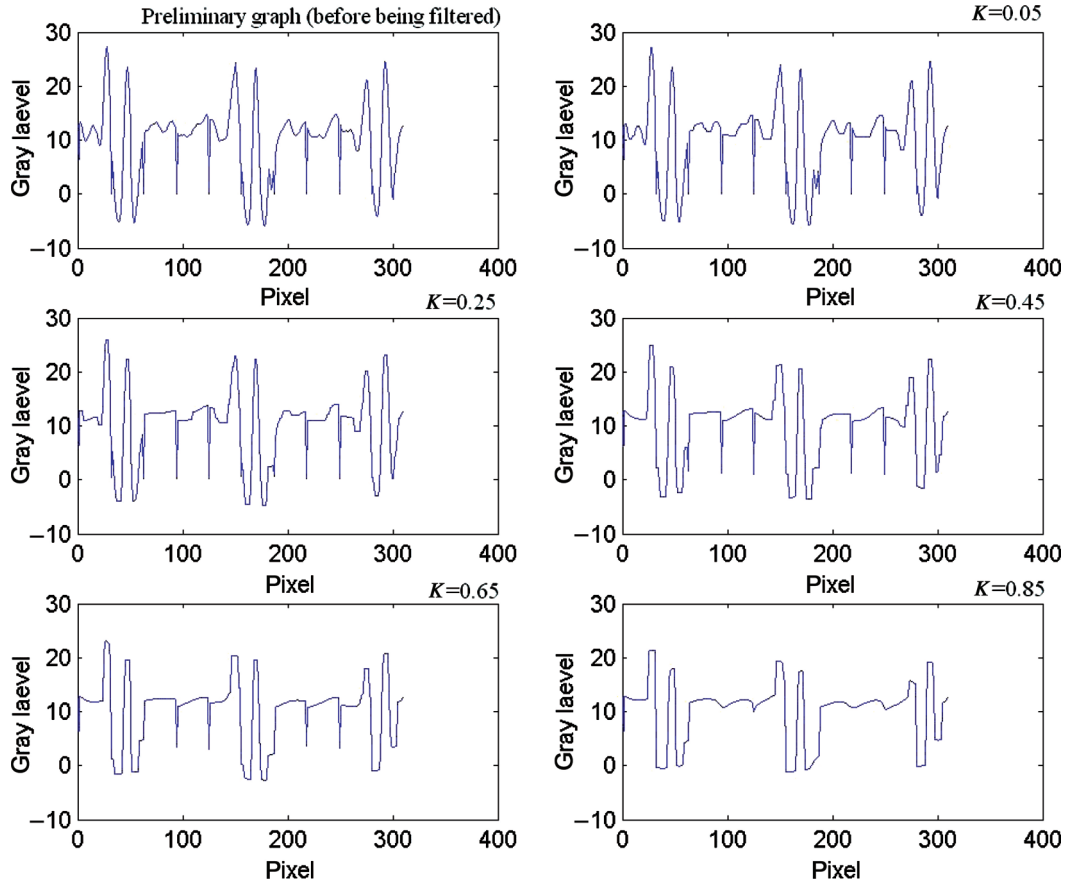


Figure 24. Variation of gray scale versus pixel as a result of applying nonlinear diffusion filters.

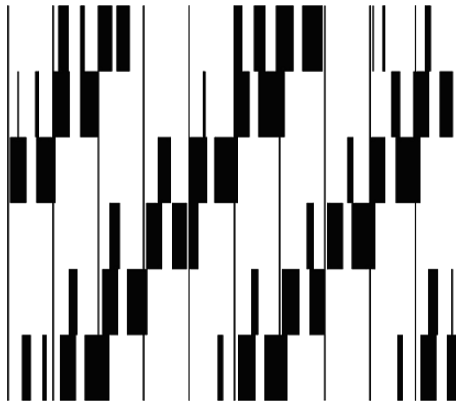


Figure 25. The preliminary weave pattern of Figure 15.

and weft points as shown in Figure 10. This is called the preliminary weave pattern.

In order to find the final weave pattern, the secondary threshold was calculated with the help of Fuzzy c-means clustering method as follows: The average of ones in each block of preliminary weave pattern was calculated and then clustered into two groups, each with a center. The average

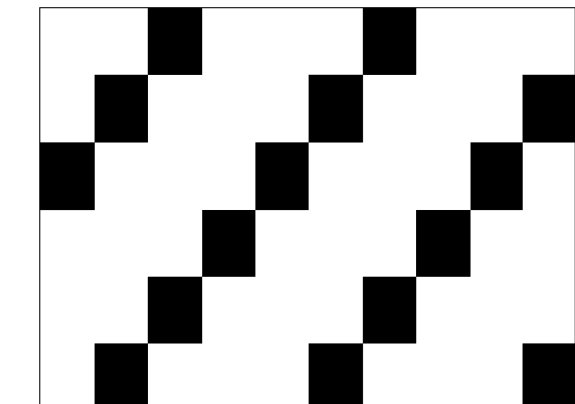


Figure 26. The final weave pattern of Figure 15.

of these two centers (here 0.6) was considered as secondary threshold. The average of ones was then compared with the secondary threshold, dividing all the blocks into two groups of smaller and bigger than the secondary threshold. This led to the formation of the final weave pattern showing the warp over weft crossing points as black squares and vice versa (Figure 11).

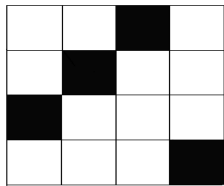


Figure 27. The weave repeat of Figure 15 (twill  $T \frac{1}{3} Z$ ).

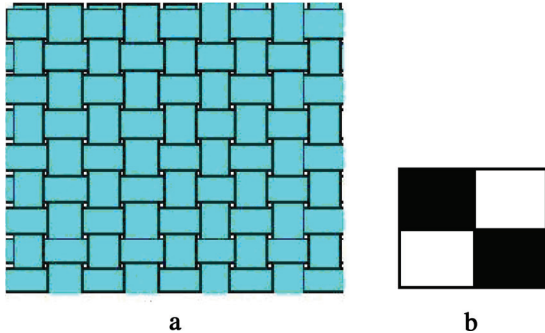


Figure 28. The original image of an ideal pattern (a) with the corresponding weave repeat (plain).

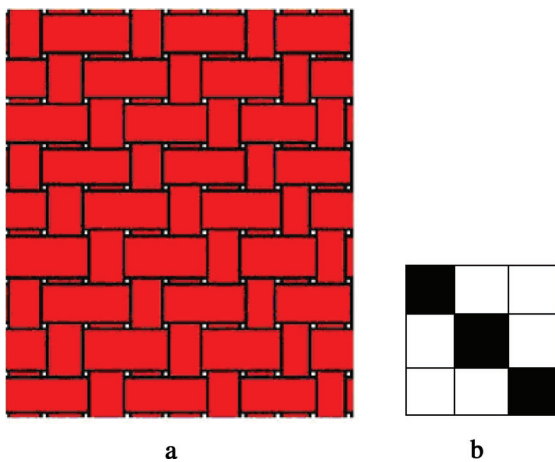


Figure 29. The original image of an ideal pattern (a) with the corresponding (b) twill weave repeat ( $T \frac{1}{2} S$ ).

Finally to identify the weave repeat, the final weave pattern was transformed into a matrix in which, zero and one replaced the black and white squares as shown in Figure 12. Then the individual rows and the columns of Figure 12 are put in a separate matrix until the first row and column are repeated (Figure 13). After converting the zeroes and ones in Figure 13 into black and white squares, the final weave repeat can be extracted as shown in Figure 14 which is satin, ( $S \frac{1}{4} Z^2$ ). It must be pointed out that for some irregular repeats that may contain two or more warps or wefts with exactly the same movement in weave repeat, the process of repeat identification will be different.

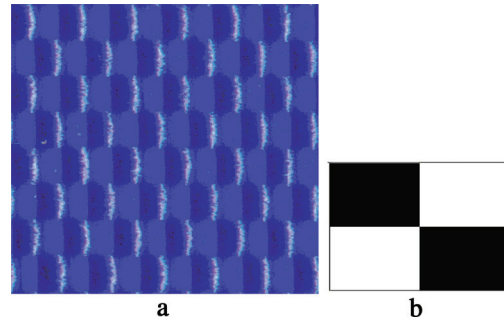


Figure 30. The scanned image (Resolution = 1200 dpi) of a real blue woven fabric. Warp (272 Tex) density = 34 per cm. Weft (272 Tex) density = 31 per cm. (b) The corresponding plain weave repeat.

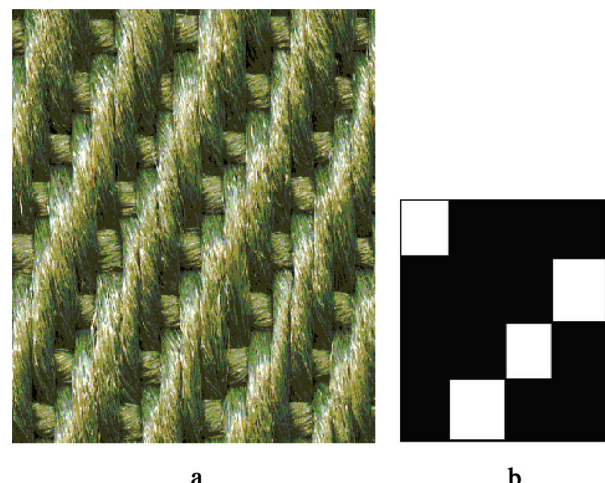


Figure 31. The scanned image (Resolution = 1200 dpi) of a real green woven fabric. Warp (1650 Tex) density = 11 per cm. Weft (1650 Tex) density = 5 per cm. (b) The corresponding twill weave repeat ( $T \frac{3}{1} Z$ ).

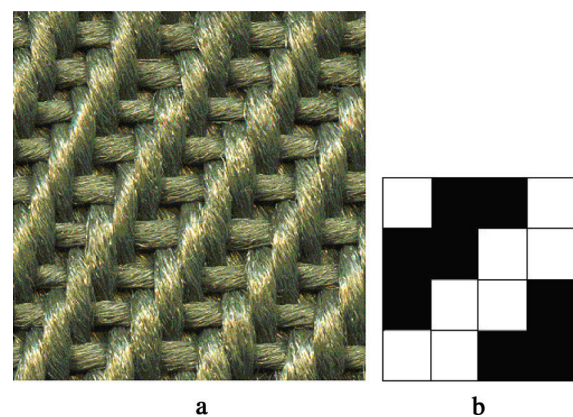


Figure 32. The scanned image (Resolution = 1200 dpi) of a real green woven fabric. Warp (1650 Tex) density = 9 per cm. Weft (1650 Tex) density = 5 per cm. (b) The corresponding twill weave repeat ( $T \frac{2}{1} Z$ ).

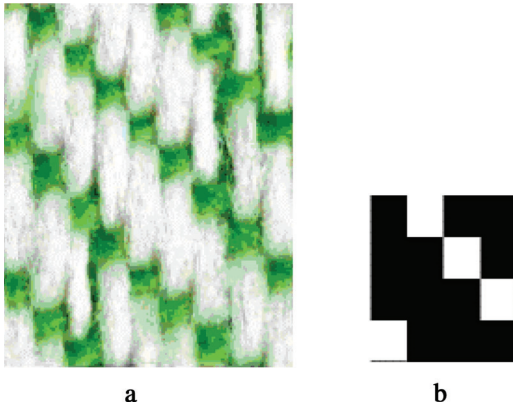


Figure 33. The scanned image (Resolution = 1200 dpi) of a real woven fabric with white warp and green weft. Warp (271 Tex) density = 14 per cm. Weft (572 Tex) density = 12 per cm. (b) The corresponding (b) twill weave repeat ( $T\frac{3}{1}S$ ).

### Real patterns

The basic approach for the identification of weave repeat of real woven fabrics is the same as ideal ones; however, as the real woven samples may suffer from defects such as loose fibers on the surface, warp and weft irregularity etc., some modifications might be necessary to make the task of weave repeat identification easier. Defects lead to different sorts of noise on the scanned image. These modifications are highlighted in the following example.

Figures 15 and 16 show the scanned image and the corresponding gray scale image of a real blue woven fabric with warp lying in the vertical direction, respectively. In order

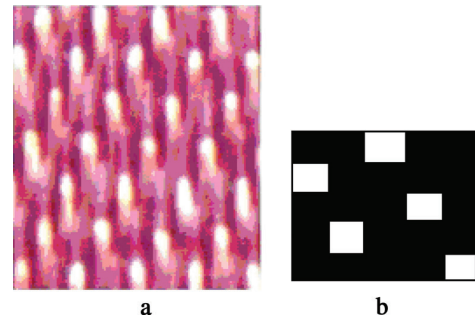


Figure 34. The scanned image (Resolution = 2400 dpi) of a real woven fabric with white warp and red weft. Warp (107 Tex) density = 96 per cm. Weft (207 Tex) density = 33 per cm. (b) The corresponding satin weave repeat ( $S\frac{1}{4}Z^3$ ).

to enhance the contrast in the gray scale image, two morphological operators, namely, top-hat and bottom-hat are employed. Figures 17 and 18 show the result of top-hat and bottom-hat being operated on the gray scale image (Figure 16). In the next stage, the top-hat operated image (Figure 17) is added to the original gray scale (Figure 16) and then the bottom-hat image (Figure 18) is subtracted from it. The result is shown in Figure 19. After this modification process, similar to the ideal images, the vertical steerable filtering is applied to the resultant gray scale image (Figure 19) and Figure 20 is obtained. Figure 20 is further blocked, resulting in Figure 21. Figure 21 is subsequently divided into sub images (Figure 22) according to the number of weft yarns (here 7) in the image. Figure 23 shows the variation of the sum of the gray scale columns versus the number of

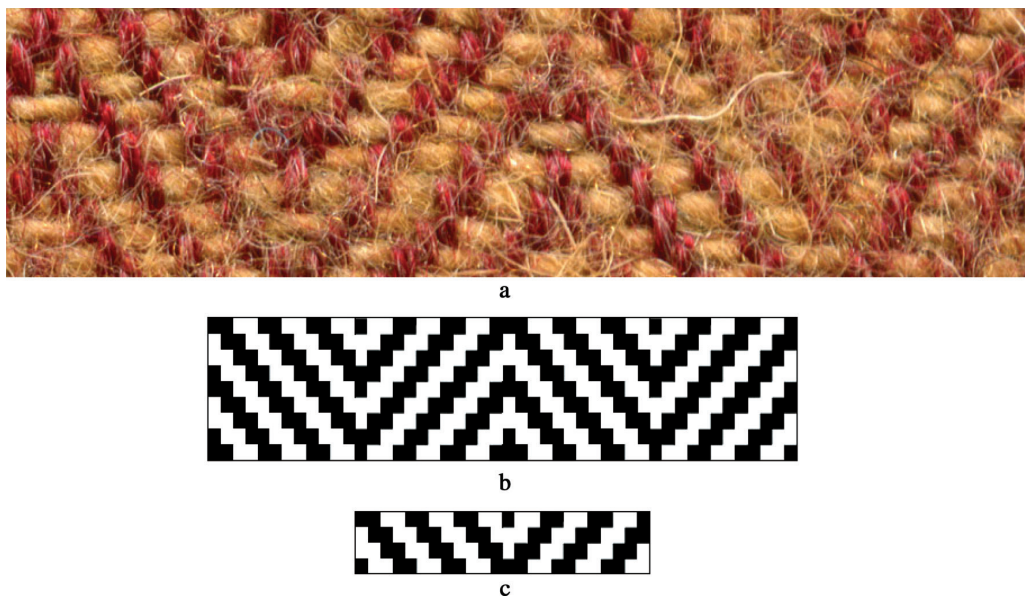


Figure 35. (a) The scanned image (Resolution = 1200 dpi) of a real woven fabric with red warp and yellow weft. Warp (350 Tex) density = 16 per cm. Weft (560 Tex) density = 12 per cm. (b) The final weave pattern of figure 35. (c) The corresponding complex weave.

pixels for the sub image shown in Figure 22. As it can be seen, recognition of the primary threshold in this case is not as easy as the case of ideal weave, shown in Figure 9. It was found that, for images of real fabrics, employing nonlinear diffusion filters leads to a more exact value for the primary threshold. Figure 24 shows the result of applying nonlinear diffusion filters for  $h_1 = h_2 = 1$  and different amounts of  $K$  ( $K = 0.05, 0.25, 0.45, 0.65$ , and  $0.85$ ). As Figure 24 shows,  $K$  values of  $0.25$  or  $0.45$  make the task of finding the value of primary threshold (about 10) easier.

In the next stage, the values of the sum matrix are compared with the primary threshold and as explained already for ideal images, the preliminary image of the weave pattern is obtained (Figure 25). Then the average value of ones in each block is compared with the calculated secondary threshold (here 0.56, the mean of two centers 0.86 and 0.26 calculated by FCM as already explained). As a result, the final weave pattern is obtained as shown in Figure 26. Finally similar to the case of ideal fabric, the weave repeat is produced. Figure 27 shows the weave repeat of Figure 15 which is twill,  $T\frac{1}{3}Z$ .

Due to space limitation, some examples, only in the form of the original image and the corresponding weave repeat as acquired by the software, obtained in this work, are shown in Figures 28–35. Figure 35 shows the scanned image of a real fabric with a complex weave. Figures 35b and c show the corresponding final weave pattern and the complex weave repeat, respectively. It must be pointed out that the identification of weave repeat from the final weave pattern is different to what already explained for basic weaves. In the case of complex (nonbasic) weaves, a separate software is needed for the identification of weave repeat (Tavanai, Palhang, Hosseini, & Moghareabed, 2006).

## Conclusion

An almost automatic method has been developed which proved being capable of identifying the weave repeat of a good variety of real fabrics tested. The tested fabrics were of one color type as well as colored yarns. Provided that the surface texture of the normal woven fabric yields a clear scanned image, the authors cannot see any difficulty for the software to identify their weave repeat. However, the software may not be applicable for cases like very high warp and weft density especially for one-color fabrics, raised fabrics, jammed structures like crepe or mock leno, and considerable skewness. Generally speaking, as there is a vast variety of weaves with possibly different textures, no universal application is claimed. It is pointed out that this algorithm was successfully applied to a fabric with a warp and weft densities of 100 threads per centimeter.

This method is based on a new algorithm. To obtain a weave repeat, the scanned image of the woven fabric is converted into gray scale and then enhanced by morphological operations. This highlights image features. Filtering by

steerable vertical filters and then segmentation into blocks showing either a warp or a weft points follows. At next stage, a matrix is made by operating sum over sub images. A primary and secondary threshold is then defined giving rise to the formation of the preliminary and final weave pattern in the form of black and white squares.

To identify the weave repeat, the black and white squares of the weave pattern are replaced by a matrix of zeroes and ones. The weave repeat is identified by finding the first repeating row and column which show the start of the next repeat vertically and horizontally, respectively.

## Acknowledgment

The authors express their sincere gratitude to Eng. Abbas Tabibi for the valuable assistance.

## References

- Bezdek, J. C. (1981). *Pattern Recognition with Fuzzy Objective Function Algorithms*, Plenum, New York.
- Bovik, A. L. (2000). *Hand book of Image and Video Processing*, Department of Electrical and Computer Engineering, Austin, Texas, pp. 433–447.
- Cui, Y. (1999). *Image Process and Analyze—Method and Application of Mathematical Morphology*, Science Press, Beijing, pp. 1–14.
- Freeman, W.T. (1992). *Steerable Filters and Local Analysis of Image Structure*. Ph.D. thesis, Massachusetts Institute of Technology, USA.
- Freeman, W.T., & Adelson, E. H. (1991). The Design and Use of Steerable Filters, *IEEE. Transactions on Pattern Analysis and Machine Intelligence*, 13(6), 891–907.
- Gonzales, R.C., & Wintz, P. (1987). *Digital Image Processing* (2nd ed.), Addison-Wesley, Canada, pp. 3–7.
- Heijmans, J.A.M. (1991). Theoretical aspects of gray-level morphology, *IEEE. Transactions on Pattern Analysis and Machine Intelligence*, 13(5), 568–582.
- Huang, C.C., Liu, S.C., & Yu, W.H. (2000). Woven Fabric Analysis by Image Processing, Part 1: Identification of Weave Patterns, *Textile Research Journal*, 70(6), 481–485.
- Jeon, B.S., Bae, J.H., & Suh, M.W. (2003). Automatic recognition of woven fabric patterns by an artificial neural network, *Textile Research Journal*, 73(7), 645–650.
- Kang, T.J., Kim, C.H., & Oh, K.W. (1999). Automatic recognition of fabric weave patterns by digital image analysis, *Textile Research Journal*, 69, 77–83.
- Kuo, C.F.H., Shih, C.Y., & Lee, J.Y. (2004). Automatic recognition of fabric weave patterns by a fuzzy c-means clustering method, *Textile Research Journal*, 74(2), 107–111.
- Lachkar, A., Benslimane, R., Dorazio, L., & Martuscelli, E. (2005). Textile woven fabric recognition using Fourier image analysis techniques: Part 2—texture analysis for crossed-states detection, *Textile Institute*, 96(3), 179–183.
- Ohta, K., Nonaka, Y., & Miyawaki, F. (1995). *Automatic analysis of a weaving design with the spatial frequency components*, Image Analysis Applications and Computer Graphics. In Proceedings of Third International Computer Science Conference, Springer-Verlag, Berlin, Germany, pp. 516, 517.
- Parker, J.R. (1997). *Algorithms for Image Processing and Computer Vision*, Wiley Computer, New York, NY, pp. 68–114.
- Pedrycz, W. (1997). Fuzzy clustering with partial supervision. IEEE transactions on systems, man, and cybernetics, part B: *Cybernetics*, 27(5), 787–795.

- Perona, P., & Malik, J. (1990). Scale-space and edge detection using anisotropic diffusion, *IEEE Transactions on Pattern Analysis and Machine Intelligence, PAMI-12*, 629–639.
- Ravandi, S.A.H., & Toriumi, K. (1995). Fourier transform analysis of plain weave fabric appearance, *Textile Research Journal*, 65(11), 676–683.
- Tavanai, H., Palhang, M., Hosseini, S.A., & Moghareabed, M. (2006). Identification of printed pattern repeat and its dimensions by image analysis, *Journal of Textile Institute*, 97(1), 71–78.
- Xu, B. (1996). Identifying fabric structures with fast Fourier transform techniques, *Textile Research Journal*, 66(8), 496–506.